

# Atomic Layer Deposition of Tantalum Oxide Thin Films from Iodide Precursor

Kaupo Kukli,<sup>\*,†</sup> Jaan Aarik,<sup>‡</sup> Aleks Aidla,<sup>‡</sup> Katarina Forsgren,<sup>§</sup> Jonas Sundqvist,<sup>§</sup> Anders Härsta,<sup>§</sup> Teet Uustare,<sup>‡</sup> Hugo Mändar,<sup>‡</sup> and Alma-Asta Kiisler<sup>‡</sup>

*Institute of Experimental Physics and Technology, University of Tartu, Tähe 4, EE-51010, Tartu, Estonia, Institute of Materials Science, University of Tartu, Tähe 4, EE-51010 Tartu, Estonia, and The Ångström Laboratory, Inorganic Chemistry, Uppsala University, P.O.Box 538, SE-75121 Uppsala, Sweden*

Received May 17, 2000. Revised Manuscript Received September 19, 2000

Atomic layer deposition (ALD) of Ta<sub>2</sub>O<sub>5</sub> films from evaporated TaI<sub>5</sub> and H<sub>2</sub>O–H<sub>2</sub>O<sub>2</sub> was investigated in the temperature range of 240–400 °C. It was shown that TaI<sub>5</sub> as a novel ALD precursor is sufficiently stable for deposition of amorphous or polycrystalline films. According to XPS, the films were free from iodine residues. The refractive index of the films reached 2.24. The film formation mechanism depended on the substrate temperature. The growth rate decreased linearly with substrate temperature. Real time monitoring of the growth process with a quartz crystal microbalance revealed the self-limiting nature of reactions between the film surface and precursors at substrate temperatures up to 325 °C. Etching of Ta<sub>2</sub>O<sub>5</sub> in the TaI<sub>5</sub> flow was observed at around 350 °C and higher temperatures. At 350 °C, the crystal growth was also initiated.

## Introduction

Ta<sub>2</sub>O<sub>5</sub> thin films are of importance as component layers in optical coatings,<sup>1</sup> solid-state ion sensors,<sup>2</sup> and metal-oxide-semiconductor transistors<sup>3–6</sup> and in dynamic memory capacitor structures.<sup>7,8</sup> The structure, thickness uniformity, conformal growth, purity, and performance of the functional oxide films depend largely on the deposition method and precursors chosen. Besides rather conventional alkoxide precursors available for chemical vapor deposition (CVD) of Ta<sub>2</sub>O<sub>5</sub>,<sup>3,9</sup> an alternative selection can also be made among halide precursors.<sup>10</sup> For instance, TaF<sub>5</sub> has been studied as an alternative carbon-free precursor.<sup>4,11</sup> Also, metal iodides fulfill the requirements for high-quality chemical precursors. Large ionic radii and relatively weak metal–

iodine bond strength are likely reasons for the high purity generally achieved in the resulting thin film structures. Iodine-free Bi<sub>2</sub>O<sub>3</sub><sup>12</sup> and Ta<sub>2</sub>O<sub>5</sub><sup>13</sup> have been obtained in halide CVD processes carried out at low temperatures, down to 300 °C. Another important quality is the phase composition of functional layers because crystalline films are usually characterized by higher dielectric permittivity<sup>14</sup> while amorphous layers provide essentially higher electrical resistance<sup>14</sup> and stability against aging.<sup>2</sup>

To attain precise thickness control and enable further decrease in the deposition temperature, while maintaining the homogeneity of the amorphous or polycrystalline films, one can apply atomic layer deposition (ALD), using the technique analogous to that developed by Suntola.<sup>15</sup> In addition to convenient thickness control, this method allows conformal growth on profiled substrates.<sup>17</sup> ALD is a modification of CVD where the precursors alternately chemisorb in the form of (sub-)monomolecular layers on the substrate surface. Metal-oxide layers can be formed by reacting an oxygen precursor, for example, H<sub>2</sub>O or H<sub>2</sub>O<sub>2</sub> with, for instance, an adsorbed metal-halide layer. The film grows as a result of sequential surface reactions, while the film thickness remains precisely determined by the number of cycles applied. During each cycle, one or less than

\* To whom correspondence should be addressed. E-mail: kaupok@ut.ee.

† Institute of Experimental Physics and Technology, University of Tartu.

‡ Institute of Materials Science, University of Tartu.

§ Uppsala University.

(1) Jakobs, S.; Duparré, A.; Huter, M.; Pulker, H. K. *Thin Solid Films* **1999**, *351*, 141.

(2) Teravaninthorn, U.; Miyahara, Y.; Moriizumi, T. *Jpn. J. Appl. Phys.* **1987**, *26*, 2116.

(3) Lai, B. C.; Kung, N.; Lee, J. Y. *J. Appl. Phys.* **1999**, *85*, 4087.

(4) Devine, R. A. B.; Chaneliere, C.; Autran, J. L.; Bolland, B.; Baillet, P.; Leray, J. L. *Microelectron. Eng.* **1997**, *36*, 61.

(5) Houssa, M.; Degraeve, R.; Mertens, P. W.; Heyns, M. M.; Jeon, J. S.; Halliyal, A.; Ogle, B. *J. Appl. Phys.* **1999**, *86*, 6462.

(6) Roy, P. K.; Kizilyalli, I. C. *Appl. Phys. Lett.* **1998**, *72*, 2835.

(7) Lai, B. C.; Lee, J. Y. *J. Electrochem. Soc.* **1999**, *146*, 266.

(8) Treichel, H.; Mitwalsky, A.; Sandler, N. P.; Tribula, D.; Kern, W.; Lane, A. P. *Adv. Mater. Opt. Electron.* **1992**, *1*, 299.

(9) Crosbie, M. J.; Wright, P. J.; Williams, D. J.; Lane, P. A.; Jones, J.; Jones, A. C.; Leedham, T. J.; O'Brien, P.; Davies, H. O. *J. Phys. IV France* **1999**, *9*, Pr8-935.

(10) Härsta, A. *Chem. Vap. Deposition* **1999**, *5*, 191.

(11) Luo, E. Z.; Sundravel, B.; Luo, H. G.; Wilson, I. H.; Four, S.; Devine, R. A. B. *J. Vac. Sci. Technol.* **1999**, *17*, 3235.

(12) Schuisly, M.; Härsta, A. *J. Electrochem. Soc.* **1998**, *145*, 4234.

(13) Forsgren, K.; Härsta, A. *Thin Solid Films* **1999**, *343–344*, 111.

(14) Shibata, S. *Thin Solid Films* **1996**, *277*, 1.

(15) Suntola, T. In *Handbook of Crystal Growth 3, Thin Films and Epitaxy, Part B: Growth Mechanisms and Dynamics*; Hurler, D. T. J., Ed.; Elsevier Science B. V.: New York, 1994; p 654.

(16) Comizzoli, R. B.; Dautartas, M. F.; Osenbach, J. W. U.S. Patent No. 5,851,849, 1997.

(17) Ritala, M.; Leskelä, M.; Dekker, J.-P.; Mutsaers, C.; Soininen, P. J.; Skarp, J. *Chem. Vap. Deposition* **1999**, *5*, 7.

one atomic layer of metal, together with the corresponding amount of oxygen, can be deposited.

So far, probably the only halide precursor systematically used for ALD of Ta<sub>2</sub>O<sub>5</sub> has been TaCl<sub>5</sub>.<sup>16,18–22</sup> The present study is aimed at the adaptation of the TaI<sub>5</sub>–H<sub>2</sub>O<sub>2</sub> precursor system for the ALD process of Ta<sub>2</sub>O<sub>5</sub> films. TaI<sub>5</sub> and aqueous solution of H<sub>2</sub>O<sub>2</sub> were applied as metal and oxygen precursors, respectively, while the growth of Ta<sub>2</sub>O<sub>5</sub> was monitored in real time using a quartz crystal microbalance (QCM). As noticed earlier,<sup>23</sup> the oxides may grow faster in iodide-based ALD when using H<sub>2</sub>O<sub>2</sub> solution instead of H<sub>2</sub>O. H<sub>2</sub>O<sub>2</sub> is known as a reagent able to complete the oxidation of multivalent metals whereas water may demonstrate insufficient reactivity, resulting in incomplete oxidation, giving a mixture of suboxides and amorphous hydroxides.<sup>24</sup> Indeed, in the case of TiO<sub>2</sub>, the water-assisted ALD resulted in the formation of suboxides or anatase–rutile mixture films growing at a relatively low rate while the application of H<sub>2</sub>O<sub>2</sub> enabled the formation of dioxide at an appreciable rate.<sup>23</sup> It is suggested that H<sub>2</sub>O<sub>2</sub> decomposes at the substrate to oxygen and water. The oxygen may complete the surface reactions while H<sub>2</sub>O mainly re-creates OH groups on the surface, being the source of active adsorption sites.

### Experimental Section

The studies were carried out in a hot-wall horizontal flow-type ALD reactor.<sup>25</sup> TaI<sub>5</sub> (Strem Chemicals Inc., 99%) was evaporated from semi-open boats located inside the reactor. H<sub>2</sub>O<sub>2</sub> (30%) was evaporated at 20 °C from a special reservoir outside the reactor. The dose of the H<sub>2</sub>O–H<sub>2</sub>O<sub>2</sub> vapor mixture was controlled by a needle valve, which allowed tuning of the partial pressure of the mixture between 0.1 and 14 Pa, approximately, in the reaction zone. N<sub>2</sub> (99.999%) was used as a carrier gas. The total pressure in the ALD reactor was 250 Pa, approximately.

The adsorption process was characterized by means of QCM with 30-MHz working frequency and 0.5-s response time. QCM was also used to study the growth rate as a function of the TaI<sub>5</sub> pulse length,  $t_1$ , the first purge time,  $t_2$ , the H<sub>2</sub>O<sub>2</sub> exposure time,  $t_3$ , the length of the second purge period,  $t_4$ , the TaI<sub>5</sub> source temperature,  $T_S$ , and the reactor (substrate) temperature,  $T_R$ . During the real-time monitoring, the QCM was placed in the reactor chamber instead of the susceptor. The mass sensor was at the same distance from the gas inlet where otherwise the leading edges of the substrates were located. To avoid possible reactions between the Ag electrodes of the QCM and oncoming iodide flux, the electrode surface was first covered with a few nanometers thick amorphous Ta<sub>2</sub>O<sub>5</sub> deposited from TaCl<sub>5</sub> and H<sub>2</sub>O at 250 °C.

Sample films were grown onto fused quartz and (100)-oriented Si substrates at 250, 300, 325, 350, and 400 °C. Prior to deposition, the native SiO<sub>2</sub> layer was removed by cleaning

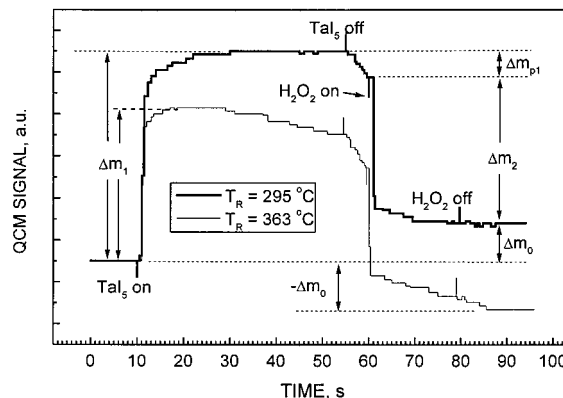


**Figure 1.** Characteristic alterations in adsorbing mass, expressed by changes in the QCM oscillation period.  $\Delta m_1$  is the mass increase during TaI<sub>5</sub> exposure.  $\Delta m_{p1}$  is the mass desorbing during the first purge period.  $\Delta m_2$  is the surface mass decrease during the surface reaction between surface TaI<sub>x</sub> species and H<sub>2</sub>O–H<sub>2</sub>O<sub>2</sub> flux.  $\Delta m_0$  is the difference between final and initial QCM output levels, expressing the mass of oxide layer deposited in this cycle.

the substrates in an aqueous solution of NH<sub>4</sub>F and HF (2%). The structure of the films was studied using reflection high-energy electron diffraction (RHEED) and X-ray diffraction (XRD) with Bragg–Brentano geometry, using Cu K $\alpha$  radiation. The residual iodine contamination level was checked by X-ray photoelectron spectroscopy (XPS) using Perkin-Elmer 5500 equipment, with Al K $\alpha$  (1486.6 eV) radiation. The detection limit for iodine by XPS was better than 0.1%. To obtain information about possible composition profiles, the films were sputtered using an Ar<sup>+</sup> ion beam with 3 keV of energy and a current density of 4  $\mu$ A/cm<sup>2</sup>. The transmission spectra of the films grown onto silica substrates were measured with a Hitachi U2000 spectrophotometer in the wavelength range of 370–1100 nm. The thickness and refractive index were calculated from these spectra, using the method developed by Ylilammi and Ranta-aho.<sup>26</sup>

### Results and Discussion

**Features of Precursor Adsorption.** To characterize the deposition kinetics, the mass sensor signal as a function of time was recorded during relatively long deposition cycles (Figure 1). During the TaI<sub>5</sub> pulse,  $t_1$ , the mass load, detected by QCM, increased and stabilized at a certain level,  $\Delta m_1$ . The stabilization of the QCM signal directly indicated the self-limiting nature of the precursor chemisorption when the surface became saturated with the species adsorbed. During the H<sub>2</sub>O–H<sub>2</sub>O<sub>2</sub> pulse, the mass decreased by the amount expressed by  $\Delta m_2$  and, after the completion of the growth cycle, the mass of the deposited oxide layer could be observed and denoted as  $\Delta m_0$ .

After saturation, the mass sensor signal remained at a stabilized level in the temperature range of 240–325 °C. At higher temperatures, a continuous decrease of mass in real time became evident in the case of sufficiently long TaI<sub>5</sub> exposure times (Figure 1). The mass decrease during the TaI<sub>5</sub> pulse was enhanced by increasing the substrate temperature and, concurrently,  $\Delta m_0$  decreased. At sufficiently long TaI<sub>5</sub> pulse times and high substrate temperatures,  $\Delta m_0$  became negative, indicating that etching reactions between TaI<sub>5</sub> and the underlying Ta<sub>2</sub>O<sub>5</sub> film influenced the process, removing

(18) Pessa, M.; Mäkelä, R.; Suntola, T. *Appl. Phys. Lett.* **1981**, *38*, 131.

(19) Aarik, J.; Aidla, A.; Kukli, K.; Uustare, T. *J. Cryst. Growth* **1994**, *144*, 116.

(20) Aarik, J.; Kukli, K.; Aidla, A.; Pung, L. *Appl. Surf. Sci.* **1996**, *103*, 331.

(21) Kukli, K.; Ritala, M.; Matero, R.; Leskelä, M. *J. Cryst. Growth* **2000**, *212*, 459.

(22) Kukli, K.; Aarik, J.; Aidla, A.; Kohan, O.; Uustare, T.; Sammelselg, V. *Thin Solid Films* **1995**, *260*, 135.

(23) Kukli, K.; Ritala, M.; Schuisky, M.; Leskelä, M.; Sajavaara, T.; Keinonen, J.; Uustare, T.; Härsta, A. *Chem. Vap. Deposition* **2000**, *6*, 303.

(24) Moon, J.; Awano, M.; Takagi, H.; Fujishiro, Y. *J. Mater. Res.* **1999**, *14*, 4594.

(25) Aarik, J.; Aidla, A.; Uustare, T.; Sammelselg, V. *J. Cryst. Growth* **1995**, *148*, 268.

(26) Ylilammi, M.; Ranta-aho, T. *Thin Solid Films* **1993**, *232*, 56.

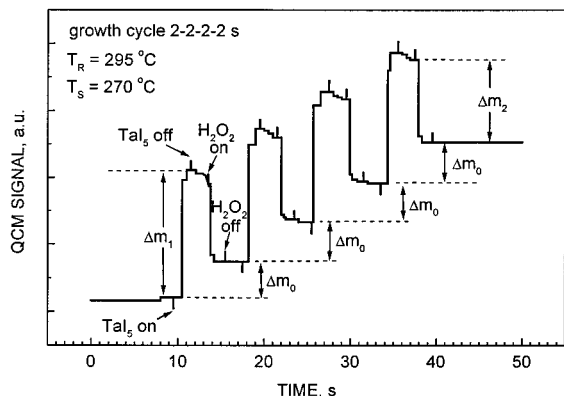


**Figure 2.** Surface mass changes, recorded in cyclic ALD film growth process in the  $\text{TaI}_5\text{-H}_2\text{O}_2$  precursor system. The label key is as that for Figure 1.

some amount of the previously deposited oxide. In the present case, the etching was still slower than that observed earlier in the  $\text{TaCl}_5\text{-H}_2\text{O}$  precursor system.<sup>19–21</sup> Nevertheless, to minimize etching effects, most of the experiments were carried out by using reasonably short pulse times. The sample films were grown using  $\text{TaI}_5$  pulses as short as 2 s. The behavior of the film mass in such a process is depicted in Figure 2. This behavior resembles that characteristic of the sequential pulsing of  $\text{TiI}_4$  and  $\text{H}_2\text{O}_2$  in the ALD of  $\text{TiO}_2$ .<sup>27</sup>

A certain mass decrease,  $\Delta m_{p1}$ , was detected during the first purge period,  $t_2$ , at any temperature studied. This effect was also quite similar to that observed in the  $\text{TiI}_4\text{-H}_2\text{O}_2$  precursor system.<sup>27</sup> The mass decrease indicated desorption or decomposition of surface species while the species released might also include etching products not removed during the  $\text{TaI}_5$  pulse.

Upon the  $\text{H}_2\text{O-H}_2\text{O}_2$  exposure during  $t_3$ , the surface mass decreased rather abruptly by  $\Delta m_2$ . This indicated that some amount of iodine ligands was released and replaced with much lighter oxygen or OH groups. The measure of the relative mass of the  $\text{Ta}_2\text{O}_5$  layer deposited in the current cycle was the difference,  $\Delta m_0$ , between initial and final sensor output levels recorded.

**Effect of  $\text{TaI}_5$  Dosing.** The concentration of  $\text{TaI}_5$  in the gas phase, regulated by the source ( $\text{TaI}_5$  evaporation) temperature,  $T_S$ , affected the deposition rate (Figure 3). The adsorption of  $\text{TaI}_5$  was quite insignificant at evaporation temperatures below 235 °C. A rapid increase in growth rate followed the increase in  $T_S$  from 235 to 245 °C. Above 245 °C, the growth rate stabilized and remained rather insensitive to further changes in  $T_S$ . During subsequent studies,  $T_S$  was kept at about 245 °C.

The amount of tantalum oxide deposited in each cycle,  $\Delta m_0$ , increased rapidly with the  $\text{TaI}_5$  pulse length,  $t_1$ , from 0.5 to 1 s (Figure 4). Upon further increases in  $t_1$ , the  $\Delta m_0$  value continued to increase but at a considerably lower rate. At the same time,  $\Delta m_0$  was not affected by other cycle time parameters. The dependence of the growth rate on  $t_1$  might be attributed to the thermal decomposition of the metal precursor. This kind of nonsaturative increase in the mass load during the metal precursor pulse has also been observed, for

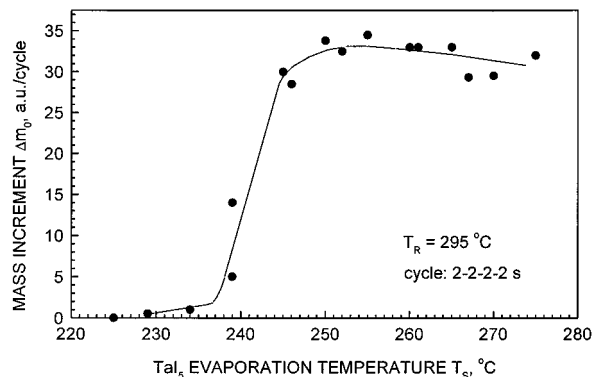


**Figure 3.** Surface mass load during a completed growth cycle,  $\Delta m_0$ , versus  $\text{TaI}_5$  evaporation temperature  $T_S$ . The solid line is a guide to the eye.

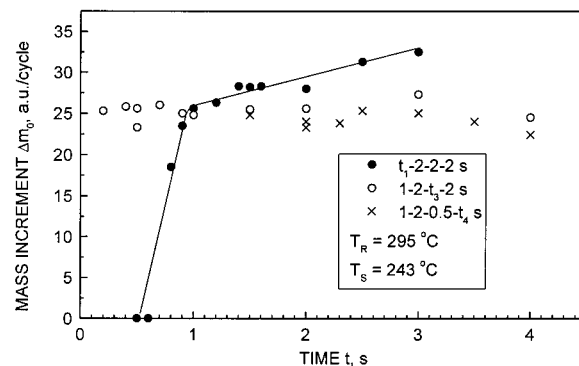


**Figure 4.** Dependence of film growth rate,  $\Delta m_0$ , measured by QCM, on the length of  $\text{TaI}_5$  pulse,  $t_1$ , on the  $\text{H}_2\text{O}_2$  exposure time,  $t_3$ , and on the length of purge period between  $\text{H}_2\text{O}_2$  and subsequent  $\text{TaI}_5$  pulses,  $t_4$ , while the first purge period,  $t_2$ , was kept constant at 2 s.

instance, in the  $\text{TiI}_4\text{-H}_2\text{O}_2$  precursor system in the temperature range of 200–400 °C<sup>27</sup> and in the  $\text{Ta}(\text{OC}_2\text{H}_5)_5\text{-H}_2\text{O}$  system at temperatures above 300 °C.<sup>28</sup> To minimize the influence of decomposition, relatively short metal precursor pulses were applied for the film growth. At the  $\text{TaI}_5$  source temperature of 270 °C,  $t_1$  values of 1–2 s provided adsorption of  $\text{TaI}_5$  close to the saturation level (Figure 4), while  $t_3$  and  $t_4$ , set at 2 s, enabled the achievement of uniform surface coverage over the substrate as long as 6 cm in the gas flow direction.

**Effect of Purging.** During the first purge period,  $t_2$ , a considerable mass decrease was observed (Figure 1). The decrease, expressed by  $\Delta m_{p1}$ , was measurable, even in the case of a relatively short purge (Figure 2), and its magnitude increased with temperature (Figure 5). The effect was attributed to the thermally enhanced release of  $\text{I}_2$ , which could have been rather easily formed as a product of precursor decomposition in iodide CVD. Indeed, experimental results confirmed that  $\Delta m_0$  was not significantly affected by  $t_2$ . Therefore, the purging process could not include desorption of Ta-containing surface species. At the same time,  $\Delta m_0$  was only weakly correlated to the growth temperature and was actually decreasing with increasing temperature (Figure 6). This indicated that the contribution of etching effects to the

(27) Kukli, K.; Aidla, A.; Aarik, J.; Schuisky, M.; Härsta, A.; Ritala, M.; Leskelä, M. *Langmuir* **2000**, *16*, 8122.

(28) Kukli, K.; Aarik, J.; Aidla, A.; Siimon, H.; Ritala, M.; Leskelä, M. *Appl. Surf. Sci.* **1997**, *112*, 236.

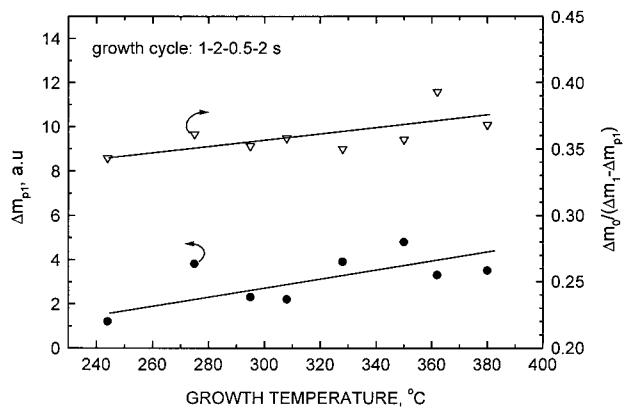


**Figure 5.** Mass desorbed during the first purge period,  $t_2$ , and the mass exchange ratio calculated,  $\Delta m_0/(\Delta m_1 - \Delta m_{p1})$ , against growth temperature. The lines are guides to the eye.

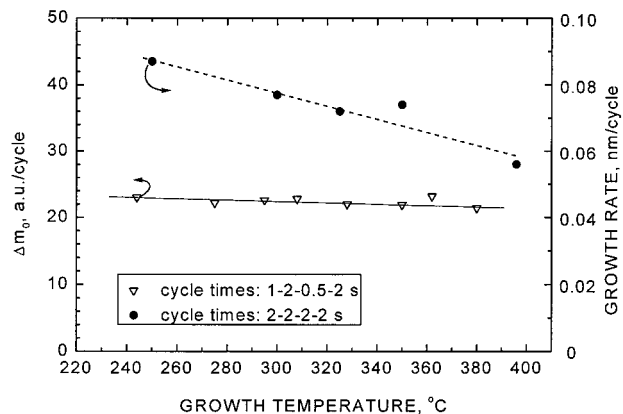


**Figure 6.** Dependence of film growth rates measured by QCM,  $\Delta m_0$  (open triangles) and calculated from the thickness optically measured (closed circles) on growth temperature. 1000 growth cycles were applied for the film deposition. The dashed line serves as a guide to the eye.

growth rate was more significant than the influence of thermal decomposition of the precursor during  $t_1$ .

Although the growth rate was rather independent of the purging length, the appropriate purge periods  $t_2$  and  $t_4$  for deposition of the sample films series were chosen as long as 2 s to ensure reliable separation of precursor fluxes and avoid an overlap between them.

**Effect of H<sub>2</sub>O–H<sub>2</sub>O<sub>2</sub> Dosing.** The length of the H<sub>2</sub>O–H<sub>2</sub>O<sub>2</sub> pulse,  $t_3$ , did not noticeably affect the growth rate (Figure 4). At the same time, the growth rate was influenced by the H<sub>2</sub>O–H<sub>2</sub>O<sub>2</sub> vapor pressure. The reduction of the partial pressure of H<sub>2</sub>O–H<sub>2</sub>O<sub>2</sub> from 14 to 0.1 Pa was accompanied by about a 30% monotonic decrease in the magnitude of  $\Delta m_0$ . At the same time, the mass deposited during TaI<sub>5</sub> exposure,  $\Delta m_1$ , was quite insensitive to the H<sub>2</sub>O–H<sub>2</sub>O<sub>2</sub> dose.

The OH groups present on the water-treated oxide surface are presumably acting as active adsorption sites for oncoming metal precursor molecules. The decrease in  $\Delta m_1$  and  $\Delta m_0$  can be explained by the decreasing density of surface OH groups at lower H<sub>2</sub>O–H<sub>2</sub>O<sub>2</sub> doses and, consequently, adsorption of lower amounts of TaI<sub>5</sub> from the gas phase by the less active substrate surface. Expectedly, the time needed for the stabilization of the QCM signal during the H<sub>2</sub>O–H<sub>2</sub>O<sub>2</sub> pulse was longer in the case of lower H<sub>2</sub>O–H<sub>2</sub>O<sub>2</sub> doses. For this reason, the H<sub>2</sub>O–H<sub>2</sub>O<sub>2</sub> dose was kept relatively high in additional

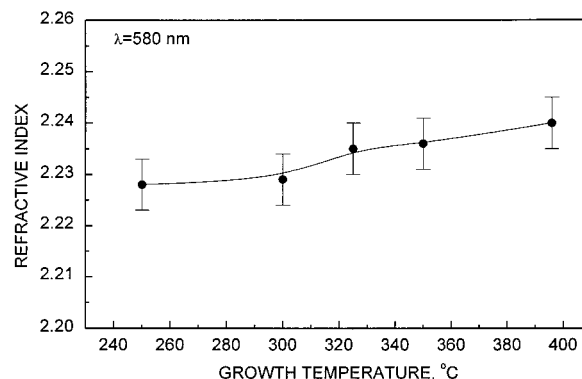


**Figure 7.** Refractive index of films, deposited on a silica substrate, against growth temperature. Pulse times used were 2–2–2–2 s. Film thicknesses ranged from 55 to 87 nm. The solid line is a guide to the eye.

experiments to ensure rapid completion of exchange reactions. However, the H<sub>2</sub>O–H<sub>2</sub>O<sub>2</sub> doses were not set at the maximum level but were kept at 8 Pa, approximately, to minimize the necessary evacuation time of H<sub>2</sub>O–H<sub>2</sub>O<sub>2</sub> vapors and avoid possible mixing of precursor pulses.

**Effect of Temperature on the Growth Mechanism.** The effect of the substrate temperature on the growth rate was determined by QCM for the cycle time sequence of 1–2–0.5–2 s set for  $t_1$ – $t_2$ – $t_3$ – $t_4$ . It can be seen that  $\Delta m_0$  decreased slightly when the substrate temperature was increased from 240 to 400 °C (Figure 6). Similar behavior of the growth rate was obtained from the series of optically determined film thicknesses. In the latter case, the values of pulse and purge times applied were 2 s. As can be seen in Figure 6, the growth rate decreased faster in the case of longer TaI<sub>5</sub> pulse times, probably due to the etching effect. At the same time, the refractive index was 2.23–2.24 and was rather insensitive to the growth temperature in the limits of experimental uncertainty (Figure 7). The bulk value of the refractive index of Ta<sub>2</sub>O<sub>5</sub> is reported to be 2.42.<sup>29</sup>

During  $t_1$ , TaI<sub>5</sub> adsorbs onto the as-deposited Ta<sub>2</sub>O<sub>5</sub> surface, exposed to H<sub>2</sub>O<sub>2</sub>–H<sub>2</sub>O flux in the preceding cycle. There is no directly measured evidence for the existence of OH groups as intermediates on this kind of Ta<sub>2</sub>O<sub>5</sub> surface. However, it is known that hydrated tantalum oxide can be formed in the hydrolysis of a tantalum halide.<sup>30</sup> On the other hand, the oxide formed may be dehydroxylated rather easily because it loses considerable amounts of OH already after heat treatment at 220–300 °C.<sup>30</sup> The existence of OH groups on a water-treated metal oxide surface has been proven, for instance, for TiO<sub>2</sub>.<sup>31</sup> Furthermore, the contact angles of water droplets on ALD-grown oxide surfaces are rather similar for TiO<sub>2</sub> and Ta<sub>2</sub>O<sub>5</sub>,<sup>32</sup> indicating similarity in their hydrophilic properties. Contact angles have been directly related to the degree of hydroxylation of an oxide surface.<sup>33</sup> The existence of OH groups is thus

(29) Black, P. W.; Wales, J. *Infrared Phys.* **1968**, *8*, 209.

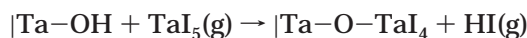
(30) Sakharov, V. V.; Korovkina, N. B.; Korshunov, B. G.; Muravlev, Yu. B. *Russ. J. Inorg. Chem.* **1983**, *28*, 1093.

(31) Haukka, S.; Lakomaa, E.-L.; Jylhä, O.; Vilhunen, J.; Horny-tzkyj, S. *Langmuir* **1993**, *9*, 3497.

(32) Utriainen, M.; Leijala, A.; Niinistö, L. *Anal. Chem.* **1999**, *71*, 2452.

(33) Takeda, S.; Fukawa, M.; Hayashi, Y.; Matsumoto, K. *Thin Solid Films* **1999**, *339*, 220.

a result of the exploitation of water while the density of OH groups should be determined by the substrate temperature and the dehydroxylation rate related to time parameters. It can be assumed that the ALD-grown oxide surface is terminated with OH groups after the end of each water pulse and subsequent TaI<sub>5</sub> may partially adsorb on the hydroxylated surface. Tantalum species remain anchored to the surface via oxygen bonds while HI is released as a product of the reaction between TaI<sub>5</sub> and OH groups. The surface reactions proceeding during the adsorption of TaI<sub>5</sub> on the surface treated with a H<sub>2</sub>O–H<sub>2</sub>O<sub>2</sub> mixture can be schematically represented as follows:



At this stage, the formation of surface TaI<sub>4</sub> species is related to the mass increment  $\Delta m_1$  (Figure 1). During the subsequent H<sub>2</sub>O–H<sub>2</sub>O<sub>2</sub> pulse, the release of the heavy iodine in the form of the volatile reaction product HI and its replacement with oxygen is reflected by the mass decrease  $\Delta m_2$ . The intermediate OH groups should be recreated in or after each reaction between adsorbed iodide species and oncoming H<sub>2</sub>O–H<sub>2</sub>O<sub>2</sub> flux. As confirmed by XPS analysis together with depth profiling carried out on the samples grown at 250, 350, and 400 °C, the films were iodine-free. The binding energies at which iodine would have been detected are 619.5 eV for 3d(5/2) and 631.0 eV for 3d(3/2) peak values. However, no XPS peaks were found at these energies. This verifies the completeness of the surface reactions between iodine-containing species and oxygen precursor H<sub>2</sub>O–H<sub>2</sub>O<sub>2</sub>. Therefore, one may assume that, during a complete ALD cycle, one TaO<sub>2.5</sub> unit is formed from each –O–TaI<sub>4</sub> surface species. In addition, as discussed above, the surface hydroxyl group involved in the formation of this –O–TaI<sub>4</sub> species should be recreated.

At any temperature, the  $\Delta m_0/\Delta m_1$  ratio can be calculated from QCM data as well as on the basis of hypothetical reaction mechanisms. In general, the exact mass balance in each reaction step should be taken into account when calculating the theoretical values of  $\Delta m_0/\Delta m_1$ . However, the molecular weight of the hydrogen species, possibly replaced during TaI<sub>5</sub> adsorption, is up to 2 orders of magnitude lower than that of the tantalum species. Therefore, experimental values of  $\Delta m_0/\Delta m_1$  ratio allow, in practice, only the estimation of the number of iodine ligands removed from a single TaI<sub>5</sub> molecule in either reaction step. For instance,  $\Delta m_0/\Delta m_1 \cong 0.32$  in the case of the reaction sequence in which four iodine ligands were bound to the adsorbed tantalum before the oxidation step.

Upon an increase in growth temperature, “polyfunctional” reactivity<sup>31</sup> between the metal precursor and surface hydroxyl groups would be enhanced and the reaction of TaI<sub>5</sub> with two or even three neighboring OH groups would become more probable, provided that the density of hydroxyl groups remains sufficiently high. However, the iodine may be released in the form of I<sub>2</sub> in the thermal decomposition process or in the form of HI when the surface intermediate species react further with neighboring OH groups. All these processes reduce the density of surface iodine and influence the growth mechanism. One can find that  $\Delta m_0/\Delta m_1 = 0.40$  when two iodine atoms are released from each TaI<sub>5</sub> molecule

adsorbed before the oxygen precursor pulse. Calculating the mass exchange ratio from the experimental QCM data recorded at different temperatures, one gets  $\Delta m_0/\Delta m_1$  values ranging from 0.330 to 0.345 without clear correlation with growth temperature. These values correspond quite well to the situation where TaI<sub>5</sub> reacts with one OH group during  $t_1$ . The contribution of bifunctional reactions, which form TaI<sub>3</sub> species attached to the surface, is possible but not so significant. The bifunctional reaction should decrease the amount of iodine in the surface species and, consequently, increase the  $\Delta m_0/\Delta m_1$  ratios. The contribution of bifunctional reactions might increase in the case of a higher amount of water flushing the substrate surface and resulting in a higher density of surface hydroxyl groups. Indeed, the experimental  $\Delta m_0/\Delta m_1$  values increased from 0.330 to 0.390 with the increase of the H<sub>2</sub>O–H<sub>2</sub>O<sub>2</sub> pressure from its minimum value to the maximum value. On the other hand, the lack of clear correlation between  $\Delta m_0/\Delta m_1$  and temperature suggests that the bifunctional reactivity is not enhanced by temperature or has only a minor effect at the oxygen precursor dose used.

Besides saturated surface reactions, there are two more processes influencing the deposition. Taking into account the temperature-enhanced decrement of surface mass density by  $\Delta m_{p1}$ , the mass exchange ratio  $\Delta m_0/(\Delta m_1 - \Delta m_{p1})$  can also be calculated and plotted against the temperature (Figure 5). Indeed, this ratio tends to increase slightly with temperature from approximately 0.34 to 0.38, indicating that, at higher temperatures, less iodine could be available for the surface reactions with H<sub>2</sub>O–H<sub>2</sub>O<sub>2</sub>. In the substrate temperature range of 300–380 °C, 3–3.5 iodine atoms per 1 Ta atom remain anchored to the surface after the first purge period. This value is somewhat lower than the I/Ta ratio described by  $\Delta m_0/\Delta m_1$  immediately after the TaI<sub>5</sub> pulse. Consequently, intermediate TaI<sub>x</sub> species should decompose thermally on the oxide surface and release iodine ligands. It is reasonable to suppose that some of these surface intermediates decompose already during the TaI<sub>5</sub> pulse, creating additional adsorption sites for oncoming TaI<sub>5</sub>.

In addition, there is an etching process during the TaI<sub>5</sub> pulse, which also affects  $\Delta m_0$ . In the etching process, volatile tantalum compounds, probably tantalum oxyiodides, leave the film surface. Data presented in Figure 1 allow one to estimate that if the TaI<sub>5</sub> pulse time was 2 s, the etching process would reduce the overall growth rate by 10%, approximately, at 360 °C and the etching rate can reach 0.05 $\Delta m_0$ /s. The contribution of etching increases with temperature. In a comparison of these results with the data presented in Figure 6, it appears that the etching effect is strong enough to cause a noticeable decrease in the growth rate with increasing growth temperature. The etching therefore compensates the possible effect of precursor decomposition, which otherwise would cause an increase in the growth rate. The etching occurring at higher temperatures, however, cannot cause the increase of  $\Delta m_0/(\Delta m_1 - \Delta m_{p1})$  because it would also result in the removal of tantalum in addition to iodine.

**Phase Composition.** The structural analysis was carried out to prove the formation of Ta<sub>2</sub>O<sub>5</sub> phases. The sample films studied were grown on substrates that

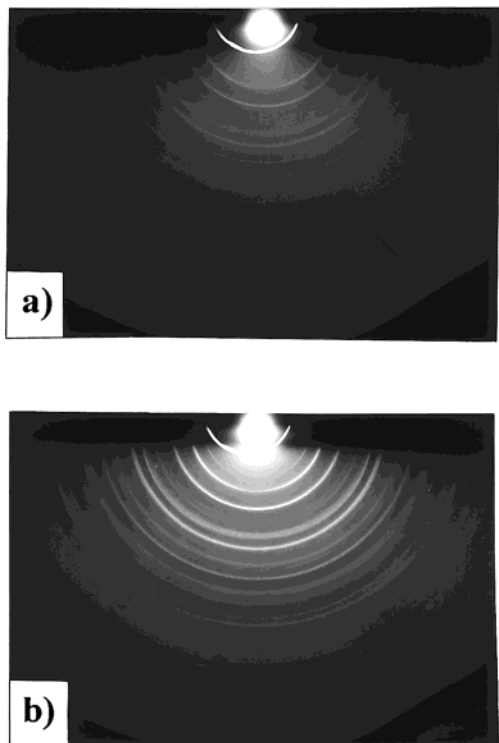


**Figure 8.** RHEED patterns of the Ta<sub>2</sub>O<sub>5</sub> films grown at 350 °C (a) and 400 °C (b) on Si(100) substrates. The thicknesses of the films were 75 and 55 nm, respectively.

were located at the leading and trailing edges of the susceptor, leaving about a 50-mm distance between substrates. The films grown on fused silica were almost entirely amorphous while those on Si(100) became partially crystallized. A phase composition profile was observed in the films along the gas flow direction. Generally, the films tended to grow more amorphous closer to the leading edge of the substrate, where the precursor fluxes arrive at the substrate surface, in comparison to the trailing edge.

RHEED analysis, describing the structure of the films with an approximate information depth of 10–20 nm, revealed the crystal structure in the films grown at temperatures not lower than 350 °C. Figure 8 demonstrates the representative RHEED patterns taken from the films grown at the leading edge of the susceptor. It can be seen that the crystallinity of the films is rather modest, owing to the high contribution from the amorphous background. The strongest lines present in the films grown at 350 °C (Figure 8a) were observed at  $d$  values of  $3.15 \pm 0.03$ ,  $2.44 \pm 0.02$ ,  $1.811 \pm 0.009$ ,  $1.65 \pm 0.009$ ,  $1.457 \pm 0.007$ , and  $1.323 \pm 0.007$  Å. These lines could be assigned to the orthorhombic  $\beta$ -Ta<sub>2</sub>O<sub>5</sub> phase ( $a = 6.20$  Å,  $b = 3.66$  Å, and  $c = 3.89$  Å),<sup>34</sup> but can equally well be assigned to either the hexagonal  $\delta$ -(Ta, O) phase ( $a = 3.624$  Å and  $c = 3.880$  Å)<sup>35</sup> or the orthorhombic L-Ta<sub>2</sub>O<sub>5</sub> phase ( $a = 6.198$  Å,  $b = 40.29$  Å, and  $c = 3.888$  Å).<sup>36,37</sup> It is to be noted that these three phases are structurally closely related. The structure

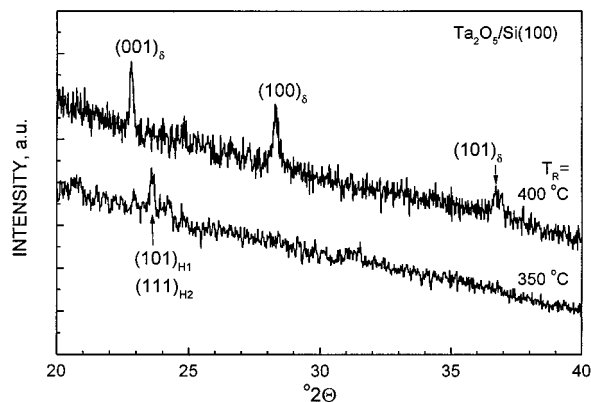


**Figure 9.** X-ray diffraction patterns of films grown at 350 and 400 °C on Si(100) substrates. The thicknesses of the films were 75 and 55 nm, respectively.

of the orthorhombic  $\beta$ -Ta<sub>2</sub>O<sub>5</sub> phase is approximately obtained from the hexagonal  $\delta$ -(Ta, O) phase by replacing the  $a$  axis of the hexagonal unit cell with  $\sqrt{3}a$  (orthorhombic  $a$  axis) and with the orthorhombic  $b$  axis equal to the hexagonal  $a$  axis. Furthermore, the structure of the orthorhombic L-Ta<sub>2</sub>O<sub>5</sub> phase is simply obtained from the orthorhombic  $\beta$ -Ta<sub>2</sub>O<sub>5</sub> phase by multiplying the  $b$  axis of  $\beta$ -Ta<sub>2</sub>O<sub>5</sub> by 11.

At a higher temperature, 400 °C, additional weak reflections appeared in the RHEED pattern (Figure 8b). These were observed at  $d$  values of  $3.89 \pm 0.03$ ,  $2.73 \pm 0.02$ ,  $2.110 \pm 0.015$ ,  $2.017 \pm 0.015$ ,  $1.625 \pm 0.009$ , and  $1.402 \pm 0.007$  Å. Only one  $d$  value (3.89) can be assigned to the  $\delta$ -phase, four to the  $\beta$ -phase, but all six to the L-Ta<sub>2</sub>O<sub>5</sub> phase. The relatively intense crystallization in the films grown at 400 °C was supported by enhanced reflection to background intensity ratio. At the same time, the role of the background was marked, resulting in that no detectable reflections could be observed, corresponding to the  $d$  values below 1 Å. Therefore, the films contained considerable amounts of amorphous phase.

At the trailing edges of the films grown at 350 °C, XRD studies with an information depth throughout the whole film revealed a weak peak at  $2\theta = 23.58^\circ$  ( $d = 3.77$  Å) (Figure 9). This peak cannot be assigned to any of the previously mentioned phases. Two monoclinic high-temperature polymorphs of Ta<sub>2</sub>O<sub>5</sub><sup>38,39</sup> are known to have a peak at this value, but definite phase identification is not possible because only one peak is clearly visible in the XRD pattern. At the same time, additional reflections were recorded at  $2\theta$  values of  $23.0$  (3.87 Å),  $28.5$  (3.13 Å), and  $36.7^\circ$  (2.44 Å) from the film grown at the trailing edge of the susceptor at 400 °C. These reflections can again be assigned to one of the three phases orthorhombic  $\beta$ -Ta<sub>2</sub>O<sub>5</sub>, hexagonal  $\delta$ -(Ta, O), or orthorhombic L-Ta<sub>2</sub>O<sub>5</sub>. In Figure 9, the peaks are assigned as those of the hexagonal oxide with respective  $d$  values 3.88, 3.14, and 2.44 Å.<sup>35</sup> The corresponding indices ascribed to the  $\beta$ -Ta<sub>2</sub>O<sub>5</sub> phase would be (001), (110), and (111) with  $d$  values of 3.87, 3.149, and 2.446 Å, respectively,<sup>34</sup> and the corresponding indices ascribed to the L-Ta<sub>2</sub>O<sub>5</sub> phase would be (001), (141), and

(34) Lehovc, K. *J. Less-Common Met.* **1964**, *7*, 397.

(35) Terao, N. *Jpn. J. Appl. Phys.* **1967**, *6*, 21; Joint Committee of Powder Diffraction Standards, Card 19-1298.

(36) Roth, R. S.; Waring, J. L.; Parker, H. S. *J. Solid State Chem.* **1970**, *2*, 445.

(37) Joint Committee of Powder Diffraction Standards, Card 25-0922.

(38) Joint Committee of Powder Diffraction Standards, Card 27-1447.

(39) Joint Committee of Powder Diffraction Standards, Card 33-1391.

(1 11 1) with  $d$  values of 3.88, 3.131, and 2.449 Å, respectively.<sup>36,37</sup> It is to be noted that the diffractograms in the case of the orthorhombic polymorphs of the stoichiometric pentoxide should contain two peaks, instead of one, close to both 28.5° and 36.7°. Such a splitting can be observed at 36.7° where, for instance, the (111) and (201) planes of  $\beta$ -Ta<sub>2</sub>O<sub>5</sub> have  $d$  values of 2.445 and 2.417 Å. However, no splitting can be observed at 28.5°. For comparison, two peaks close to 28.5°, unambiguously attributable to the orthorhombic polymorph, could be observed in the films deposited in the chloride ALD process.<sup>21</sup>

The hexagonal tantalum oxide has frequently been observed in Ta<sub>2</sub>O<sub>5</sub>-based dielectric layers.<sup>9,22,40,41</sup> Although the existence of hexagonal stoichiometric Ta<sub>2</sub>O<sub>5</sub> has recently been theoretically predicted,<sup>42</sup> both monoclinic and hexagonal Ta<sub>2</sub>O<sub>5</sub> have also been structurally described as layered, defective materials owing to the deficiency of atoms in both metal and oxygen sublattices.<sup>43,44</sup> The low-temperature hexagonal tantalum oxide may be induced by deviations from pentoxide stoichiometry and could thus be considered as an intermediate formed during tantalum oxidation and following transformation from tetragonal suboxides or amorphous phase to  $\beta$ -Ta<sub>2</sub>O<sub>5</sub>.<sup>36,43,45</sup> The formation of such a transitional intermediate in the oxidation process may be favored by intermittent changes in stoichiometry during layer-by-layer (ALD) growth at low temperatures.

An essential feature is that the Ta<sub>2</sub>O<sub>5</sub> crystal growth in the TaI<sub>5</sub>-based process seems to be significantly affected by the choice of substrate, being suppressed on fused quartz as observed in this study and enhanced on silicon substrates (Figure 9) and especially on platinum,<sup>46</sup> where the orthorhombic  $\beta$ -phase was unambiguously identified. The films grown on Si and SiO<sub>2</sub> were completely amorphous when grown below 350 °C, while a mixture of amorphous and crystalline phases were grown above this temperature.

#### Comparison between TaI<sub>5</sub>- and TaCl<sub>5</sub>-Based ALD.

The results indicate that dominantly crystalline tantalum oxide grows in both iodide and chloride ALD at

elevated temperatures. In the chloride ALD process, tetragonal suboxide (TaO<sub>2</sub>) reflections have sometimes been detected,<sup>22</sup> especially at the film surface, but none were detected in this study. On the other hand, the films grown from the iodide tended to be more amorphous than those deposited from the chloride.

In the films grown in the present study, no signal from iodine residues were detected by XPS, regardless of the deposition temperature. For comparison, earlier studies on ALD from TaCl<sub>5</sub> and H<sub>2</sub>O revealed the chlorine content as high as 0.5 at. % in films deposited at 300 °C.<sup>22</sup> Thus, it can be concluded that the concentration of residual impurities is lower in the TaI<sub>5</sub>-based ALD process, when deposited at comparable temperatures.

It is noteworthy that the etching of Ta<sub>2</sub>O<sub>5</sub> in the TaI<sub>5</sub> flow started at 350 °C, where also initial crystallization started. Thus, similarly to the case of TaCl<sub>5</sub>-based ALD,<sup>19–22</sup> the critical temperatures for the crystallization and etching of the tantalum oxide films obviously coincided. At the same time this critical temperature in the TaI<sub>5</sub> process was approximately 50 °C higher than that in the TaCl<sub>5</sub>-based process. This may be connected to the larger size and mass of iodo ligands, compared to chloro ligands, which can affect the surface diffusion rate and mobility, suppressing the nucleation. In addition, it is possible that the chlorine-containing surface species may have a higher volatility compared to the iodine-containing species, enhancing the surface migration. The chlorine-containing species should, then, be desorbed relatively easily, which reduces the threshold for the etching process. Lower threshold temperatures for the etching by TaCl<sub>5</sub>, compared to TaI<sub>5</sub>, can also be explained by more aggressive reactions between chloride and oxide.

The results of the present study demonstrated that, besides TaCl<sub>5</sub>, TaI<sub>5</sub> can be used reliably and reproducibly as a metal precursor in the halide atomic layer deposition of Ta<sub>2</sub>O<sub>5</sub> thin films. The resulting films contained different Ta<sub>2</sub>O<sub>5</sub> polymorphs and were characterized by actually higher purity than the films processed from TaCl<sub>5</sub>.

**Acknowledgment.** The authors are grateful to Mr. Torvald Andersson from the Department of Inorganic Chemistry at Uppsala University for the XPS analysis. Dr. Mikko Ritala and Prof. Markku Leskelä from the University of Helsinki are thanked for the access to transmission spectrophotometry equipment and fitting program. The study has been partially supported by the Swedish Institute and Estonian Science Foundation (Grants 4205 and 3999).

CM001086Y

(40) Kukli, K.; Ritala, M.; Leskelä, M. *J. Appl. Phys.* **1999**, *86*, 5656.

(41) Chaneliere, C.; Four, S.; Autran, J. L.; Devine, R. A. B. *Electrochem. Solid State Lett.* **1999**, *2*, 291. Chaneliere, C.; Autran, J. L.; Devine, R. A. B. *J. Appl. Phys.* **1999**, *86*, 480.

(42) Fukumoto, A.; Miwa, K. *Phys. Rev. B* **1997**, *55*, 11155.

(43) Khitrova, V. I.; Klechkovskaya, V. V. *Sov. Phys. Crystallogr.* **1980**, *25*, 669. Khitrova, V. I.; Klechkovskaya, V. V.; Pinsker, Z. G. *Sov. Phys. Crystallogr.* **1979**, *24*, 537.

(44) Khitrova, V. I.; Klechkovskaya, V. V.; Pinsker, Z. G. *Sov. Phys. Crystallogr.* **1976**, *21*, 535.

(45) Stephenson, N. C.; Roth, R. S. *Acta Crystallogr. B* **1971**, *27*, 1037.

(46) Forsgren, K.; Sundqvist, J.; Härsta, A.; Kukli, K.; Aarik, J.; Aidla, A. Fifteenth International Conference on Chemical Vapor Deposition: CVD XV, Toronto, May 14–18, 2000; Abstract No. 907.